

# SMALL WHISKBROOM IMAGER FOR ATMOSPHERIC COMPOSITION MONITORING (SWING) FROM AN UNMANNED AERIAL VEHICLE (UAV)

A. Merlaud<sup>1</sup>, D.-E. Constantin<sup>2</sup>, F. Mingireanu<sup>3</sup>, I. Mocanu<sup>4</sup>, C. Fayt<sup>1</sup>, J. Maes<sup>1</sup>, G. Murariu<sup>2</sup>, M. Voiculescu<sup>2</sup>, L. Georgescu<sup>2</sup>, and M. Van Roozendael<sup>1</sup>

<sup>1</sup>Belgian Institute for Space Aeronomy (BIRA-IASB), Avenue Circulaire 3, 1180 Brussels, Belgium (alexism@oma.be)

<sup>2</sup>University of Galati, 111 Str. Domneasca, 800008, Galati, Romania

<sup>3</sup>Romanian Space Agency (ROSA), 21-25 Str. Mendeleev, 010362, Bucharest, Romania

<sup>4</sup>Reev River Aerospace, 21 Str. Stiintei, 800146, Galati, Romania

## ABSTRACT

We describe a new instrument, the Small Whiskbroom Imager for atmospheric composition monitoring (SWING), and its first test flight on a dedicated Unmanned Aerial Vehicle (UAV). One important objective is the mapping of NO<sub>2</sub> columns at high spatial resolution allowing to subsample satellite measurements within the extent of a typical ground pixel. Simulations show that tropospheric NO<sub>2</sub> columns can possibly be monitored at a ground resolution of 200x200 m<sup>2</sup> in polluted zones. The instrument is based on a compact ultra-violet visible spectrometer and a scanner to achieve whiskbroom imaging of the trace gases fields. Including the housing and the electronics, the weight, size, and power consumption of the SWING payload are respectively 920 g, 27x12x12 cm<sup>3</sup>, and 6 W. The custom-built UAV wingspan is 2.5 m and can reach an altitude of 3 km during 2 hours, flying at 100 km/h in preprogrammed tracks. Considering the 120° swath of the instrument, it is able to cover an area of 20x20 km<sup>2</sup> in less than one hour. The spectra are analyzed using Differential Optical Absorption Spectroscopy (DOAS). Several atmospheric species are detectable in the spectral range covered by the spectrometer (250-750 nm). Water vapor, ozone, and O<sub>4</sub> have been identified in the spectra recorded during the test flight, which took place on 11 May 2013 near Galati, Romania. From this experiment, the detection limit of the SWING-UAV observation system for NO<sub>2</sub> is estimated to lie around 2 ppb, as expected from the simulations. Beside the validation of air quality satellite or local chemistry and transport models, other potential applications include monitoring NO<sub>2</sub> and/or SO<sub>2</sub> emissions from power plants, industries, ships, or volcanoes.

Key words: DOAS; Imaging; UAV; air quality.

## 1. SCIENTIFIC RATIONALE

Several instruments have already been described which achieve trace gases mapping from traditional aircraft in the UV-visible range [6, 16, 14]. These measurements are based on the Differential Optical Absorption Spectroscopy (DOAS) technique [13]. They are valuable compared to ground-based mobile DOAS experiments, which only measure horizontal gradients along roads (e.g. [2]). Airborne measurements also offer a much finer spatial resolution when compared to spaceborne sensors. For instance, [14] derived maps of tropospheric NO<sub>2</sub> over Zurich at a resolution 50x120 m<sup>2</sup> using the Airborne Prism Experiment (APEX), while the best satellite instrument in this respect is currently the Ozone Monitoring Instrument (OMI, [8]), whose pixels are 13x24 km<sup>2</sup> (13x12 km<sup>2</sup> in zoom mode). For short-lived species like NO<sub>2</sub>, the coarse resolution of satellite data actually yields representativity problems in validation exercises with ground-based measurements. This problem can be reduced using an aircraft covering a pixel extent in a relatively short time. Beside satellite validation, airborne instruments are valuable to study the accuracy of local chemistry and transport models (see Fig. 1 for such a model above the Antwerp urban area) and monitor NO<sub>2</sub> and SO<sub>2</sub> emissions from point sources such as power plants and industries [6] or ships [1].

We have developed such a payload for trace gases imaging, but from an Unmanned Aerial Vehicle (UAV). The latter has been built in parallel and we are currently investigating the capabilities of this new observation system for atmospheric research. The instrument, namely the Small Whiskbroom Imager for atmospheric composition monitoring (SWING) has already been tested from an ultralight aircraft in 2012 and from the UAV in May 2013. The Belgian Institute for Space Aeronomy (BIRA-IASB) has been interested on atmospheric measurements from UAV for some years [5] and has recently performed airborne DOAS experiments from traditional aircraft [11, 12]. SWING-UAV originates from the experience gained with these airborne DOAS systems and from the opportunity of using a dedicated UAV platform,

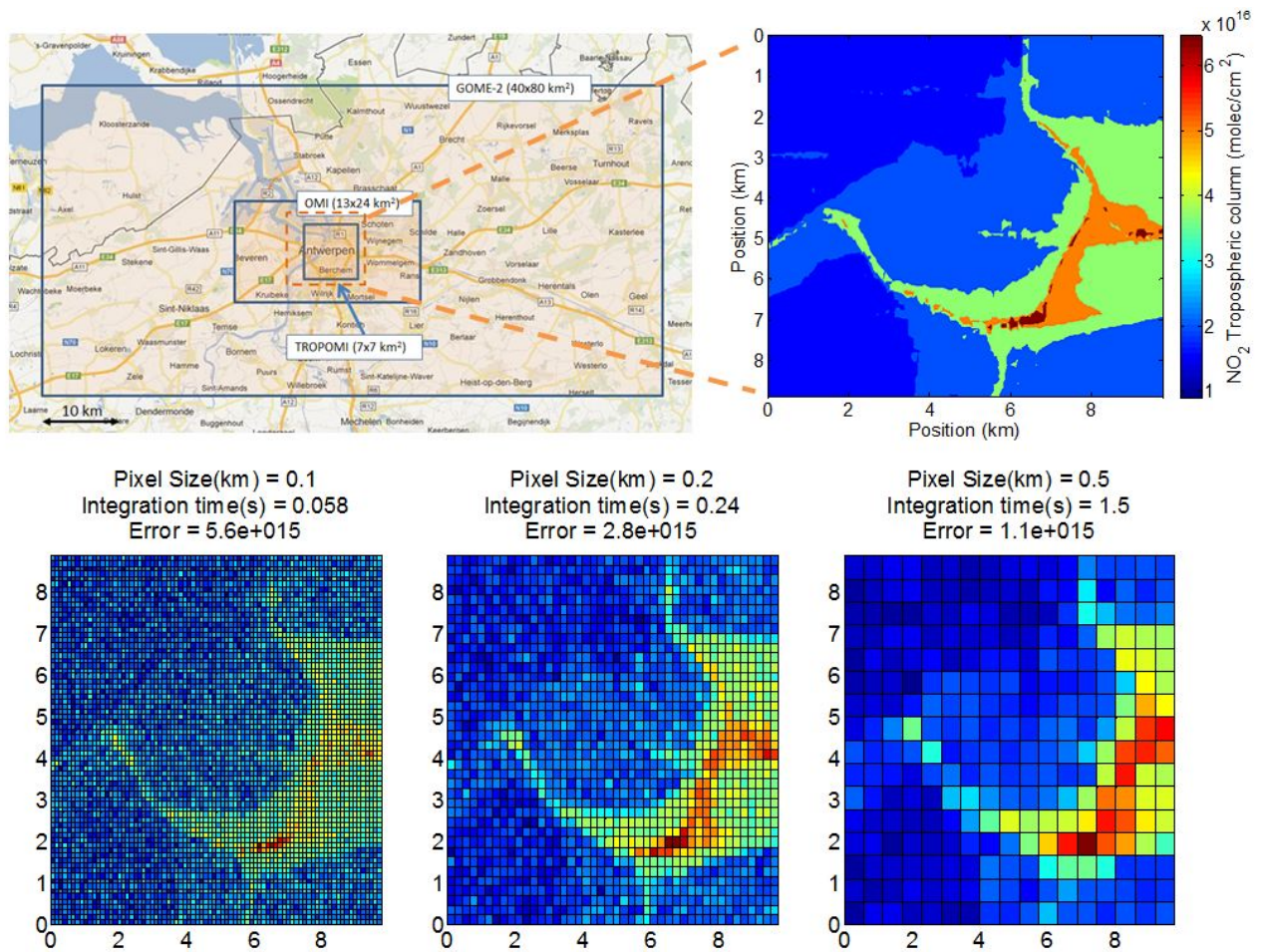


Figure 1. Simulations of NO<sub>2</sub> observations from an UAV flying at 3 km at different pixel size. The figure illustrates the trade-off between the ground resolution and the signal-to-noise ratio. Also shown are the pixel extents from current (GOME-2, OMI) and near-future (TROPOMI) satellite instruments, and the model field used as an input in the simulations.

which was made possible through the collaboration with the University of Galati. An advantage of operating from a UAV compared to a manned aircraft is the cost efficiency. The platform can also fly at lower altitudes and in hazardous environment such as inside a volcanic plume. Another whiskbroom instrument has recently been operated from a UAV for DOAS measurements, the Airborne Compact Atmospheric Mapper (ACAM, [7]). It has already measured  $\text{NO}_2$ , formaldehyde, and even tropospheric ozone above Houston. However, the platform used (the NASA Global Hawk, 40 m wingspan) is much larger than our flying wing (2.5 m wingspan) and the ACAM payload itself is over 20 kg, compared to the 900 g of SWING.

The next section presents initial simulations on the possible ground resolution of a whiskbroom imager operated from a UAV. Sect. 3 describes the hardware of the SWING instrument and the UAV platform. Sect. 4 presents the results of our first UAV test flight. Finally, Sect. 5 sums up lessons learned and states the near-future developments and perspectives for the SWING-UAV observation system.

## 2. INVESTIGATIONS ON THE ACHIEVABLE GROUND RESOLUTION

We performed simulations of  $\text{NO}_2$  measurements above a polluted zone, namely the Antwerp agglomeration in Belgium, to estimate a realistic ground resolution of a whiskbroom system from a UAV at 3 km. High resolution  $\text{NO}_2$  field forecasted around this area were taken from the PROMOTE air quality forecast service<sup>1</sup>, which is based on the Immission Frequency Distribution Model (IFDM,[3]). Only surface concentrations were available so the columns were roughly built assuming an homogeneous boundary layer of 500 m.

The relationship between the pixel size ( $P_s$ ) and the integration time ( $\tau_D$ ) used in these simulations is as follow:

$$\tau_D = \frac{P_s^2}{vS} \quad (1)$$

where  $v$  is the speed of the aircraft and  $S$  is the swath. They were set in these simulations to 60 km/h and  $120^\circ$ , respectively. This does not take into account the panoramic distortion for instance, which leads to larger pixels at the end of the swath. The objective of the simulations is to estimate the level of horizontal details due to the trade-off between spatial resolution and signal-to-noise ratio.

The baseline for the measurement noise was derived from a previous airborne experiment with the compact spectrometer used in SWING [12]. The typical error on the fitted  $\text{NO}_2$  DSCD was scaled for the shorter integration

<sup>1</sup><http://promote.vito.be/webtool/>

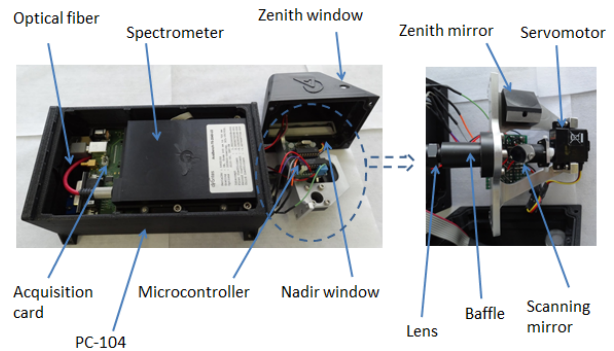


Figure 2. The SWING instrument. The size is  $27 \times 12 \times 12 \text{ cm}^3$  for 920 g, the power consumption is 6 W at 5 V. The right panel shows the scanning system in more details.

times and for the different geometry assuming photon-noise limited conditions and using relative intensities calculated with the UV-Spec/DISORT radiative transfer model [9].

Fig. 1 presents the  $\text{NO}_2$  model field used as an input and corresponding simulated observations for three different ground resolutions: 100 m, 200 m, and 500 m. The figure also shows, for a comparison, the pixel size of the current and near-future satellites GOME-2 ( $80 \times 40 \text{ km}^2$ ), OMI ( $80 \times 40 \text{ km}^2$ ), and TROPOMI ( $7 \times 7 \text{ km}^2$ ). An interesting pattern for its horizontal gradients is the South West part of the Antwerp ring-road. It appears in the model field highly polluted and it is surrounded by cleaner areas. According to the simulations, the noise level for a 100 m pixel still enables to distinguish the road from the background. In comparison, for a 500 m pixel, the image is much less noisy but the small scale of the road is almost completely diluted in the broader pixels. In real conditions, flying directly above such a perfect  $\text{NO}_2$  source may be difficult in the near-future due to clearances reasons. The intermediate value of 200 m for the ground resolution below the aircraft represents thus, from these simulations, a good compromise.

## 3. INSTRUMENT AND PLATFORM DESCRIPTION

### 3.1. The SWING payload

Fig. 2 shows the SWING instrument with its open housing. It is based on an Avantes AvaSpec-2048 spectrometer, with a  $50 \mu\text{m}$  entrance slit and a  $600 \text{ l/mm}$  grating. It covers the spectral range from 250-750 nm at a resolution of approximately 1.2 nm Full Width at Half Maximum (FWHM). Light is collected by a  $400 \mu\text{m}$  diameter optical fiber and a lens facing a mirror installed on a servomotor shaft. The mirror scans at  $\pm 60^\circ$  in the nadir direction. The instantaneous and angular field of view (FOV) are  $2.5^\circ$  and  $120^\circ$ , respectively. It is also possible to record

Table 1. Main characteristics of the SWING-UAV observation system.

SWING	Size	27x12x12 cm <sup>3</sup>
	Weight	920 g
	Power consumption	6 W
	Angular FOV	120°
	Instantaneous FOV	2.5°
UAV	Ceiling	3 km
	Wingspan	2.5 m
	Speed	60-130 km/h
	Autonomy	2 h
SWING-UAV	Pixel size	200 m
	Detection limit (NO <sub>2</sub> )	2 ppb



Figure 3. The Unmanned Aerial Vehicle built by Reev River Aerospace and dedicated to the SWING payload.

spectra in the zenith direction by rotating the scanning mirror at 90° relatively to nadir, pointing to a zenith mirror. This possibility is useful to estimate the contribution of the total column of NO<sub>2</sub> which lies above the platform. A PC-104 controls the spectrometer and the motor, the latter via a driving circuit based on a microcontroller. A GPS antenna is also connected to the PC. The whole system is powered by 5V, which is supplied by a compact battery. Considering the application, the optical windows are not in BK7 or fused silica glass but in a plastic material suitable for optical applications (Zeonex). Except the scanner support which is aluminium made, the structural parts and the housing are in plastic material (ABS). They were manufactured by 3d printing to optimize their weight and shape. More technical details about the electronics circuits and other miniaturization effort are given in [10].

Everything included, the weight, size and power consumption of SWING are respectively 920g, 27x12x12 cm<sup>3</sup>, and 6W.

### 3.2. The custom-built UAV

Fig. 3 shows the UAV dedicated to the SWING payload. The latter is fixed on the back of the aircraft, in measurement position. This UAV was customly-built for the



Figure 4. Flight tracks of the UAV test flight in Romania.

experiment by Reev River Aerospace. It is an electrically powered flying wing, with a wingspan of 2.5 m and it can reach an altitude of 3 km during 2 hours. The aircraft equipment includes attitude sensors, whose accuracy is around 0.1°, a GPS, and a steerable camera. All of these instruments are accessible through the radio during the flight, and logged four times a second. SWING being powered by its own battery, the platform and the payload are currently completely independent. Take off is achieved with a catapult and the whole flight can be preprogrammed and controlled with an autopilot. The ground segment is mainly composed of a radio antenna and a computer, and the whole set-up is easily transportable in a normal car.

## 4. RESULTS FROM THE UAV TEST FLIGHT

The first flight with the SWING instrument on the UAV took place on 11 May 2013, 15 km NW of Galati, Romania (45.53°N, 27.9°E, 95 m.a.s.l.). The aircraft took off at 7h30 UT and landed at 9h10 UT, in clear sky conditions. Fig.4 shows the flight pattern, which consisted of loops at 420 to 450 m.a.s.l, around predefined waypoints. The attitude variation during the flight are visible on Fig.6. The instrument did not stop neither at take off nor at landing. The wind was blowing from the NE direction.

Fig. 5 presents some DOAS fits of the spectra collected during the flight, performed with the QDOAS software [4]. The DOAS analysis settings used for the retrievals are similar to a previous airborne experiment with the same spectrometer [12]. Spectral signatures of four different absorbers, namely NO<sub>2</sub>, water vapor, O<sub>3</sub> and O<sub>4</sub> are clearly identified. However, the reference spectrum was recorded in Brussels and therefore the negative NO<sub>2</sub> differential slant column density (DSCD) corresponds to

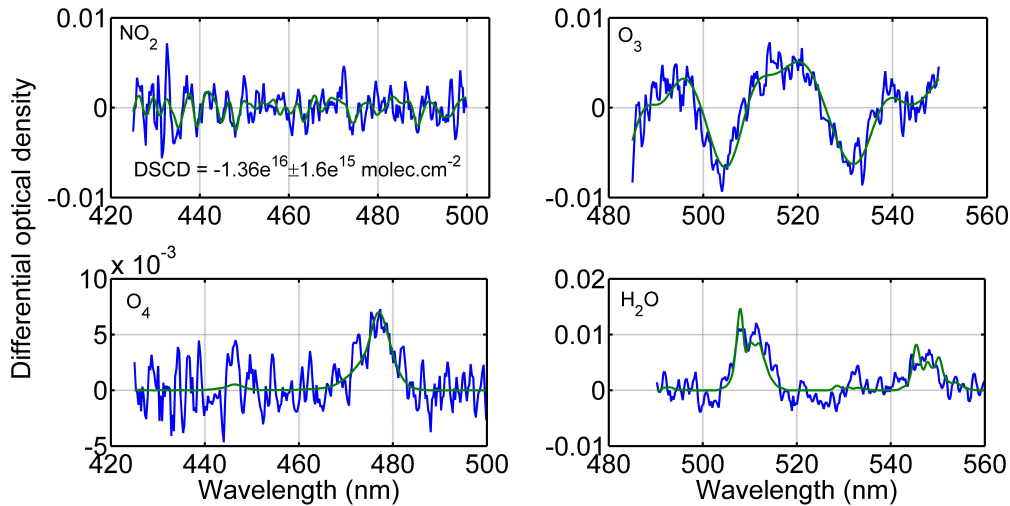


Figure 5. Examples of DOAS fits of  $\text{NO}_2$ , ozone,  $\text{O}_4$ , and water vapor, from the spectra recorded during the UAV test flight.

a larger absorption of  $\text{NO}_2$  in the reference spectrum than in the spectrum from the flight.

From the  $\text{NO}_2$  DOAS fit, it is possible to estimate a detection limit for the  $\text{NO}_2$  vertical column and volume mixing ratio (vmr). The uncertainty on the DSCDs retrieved from the spectra is estimated from the DOAS analysis to lie around  $2 \times 10^{15} \text{ molec.cm}^{-2}$  ( $1\sigma$ ). The air mass factor in nadir geometry is around 2 (see lowest panel in Fig. 6). The minimum vertical column that can be detected with the SWING-UAV is thus  $1 \times 10^{15} \text{ molec.cm}^{-2}$ . Assuming a 500 m well-mixed boundary layer, this column corresponds to a vmr of 0.8 ppbv. The  $2\sigma$  detection limit in vmr can thus be conservatively estimated to 2 ppbv. This value could be further reduced when flying at a higher altitude, but the actual detection limit depends also on the weather conditions and solar zenith angles.

Besides checking the quality of the spectra, the test flight enabled us to study the attitude stability during the flight. Fig. 6 presents an excerpt of the time series focusing on the measurement geometry. Starting from the top, the first panel shows the angle of the scanner relative to nadir. The second presents the pitch and roll angles of the aircraft. The elevation of the scanner compared to the ground (third panel,  $0^\circ$  corresponds to nadir) is calculated combining these two angles with the heading direction, following [15]. The largest elevation angles with respect to the nadir direction corresponds to the time periods when the UAV is changing heading direction, which are in fact more visible in the roll angle time series. Focusing on the period when flight is straight, the pitch and roll stay within  $\pm 10^\circ$ .

The lowest panel of Fig. 6 presents air mass factor (AMF) calculations based on the measured attitudes and heading direction of the panels above, but for observations at 3 km. The AMFs corresponding to two different ground albedos are presented. We used the radiative transfer code UV-Spec/DISORT [9], with the same well-mixed bound-

ary layer assumption. The solar azimuth angle was set to  $45^\circ$ . Interestingly, the AMF appears quite stable with the scan angle, at least when the scan elevation is below a threshold at around  $65^\circ$ . Under this value, the AMF varies weakly ( $\pm 10\%$ ) with the scan elevation. Large variations of the AMF (50%) are only observed when the scan elevation is above  $65^\circ$ , i.e. when the UAV is changing direction. This finding reduces the importance of the pointing error for the AMF calculation. By contrast, the figure points out the importance of using a correct albedo for the AMF estimation since the effect of this parameter appears important for the absolute value of the AMF.

## 5. CONCLUSIONS AND PERSPECTIVES

A miniaturized instrument for trace gases mapping from a UAV was developed. Everything included, the weight, size and power consumption of SWING are respectively 920g,  $27 \times 12 \times 12 \text{ cm}^3$ , and 6W. The first test flight on the custom-built UAV took place in Romania on 11 May 2013. Water vapor, ozone, and  $\text{O}_4$  were identified in the spectra, whereas  $\text{NO}_2$  detection limit could be estimated at 2 ppbv. We also started to investigate the AMF calculations for the considered geometry. This step will be necessary to convert the DSCDs retrieved with the DOAS analysis to more geophysically relevant vertical columns. Our findings indicate that the pointing error appears negligible compared to the albedo effect.

Some work is ongoing to improve the capabilities of the SWING-UAV observation system. First, the scanning loop will be optimized, to increase the number of points per scan (upper panel, Fig. 6). This is important to increase the ground cover of the measurements. The angular offsets between the attitude sensor and the scanner will be characterized accurately. Indeed, if the pointing error is not important for the AMF calculation, it plays a great role for the georeferencing issues. Other charac-

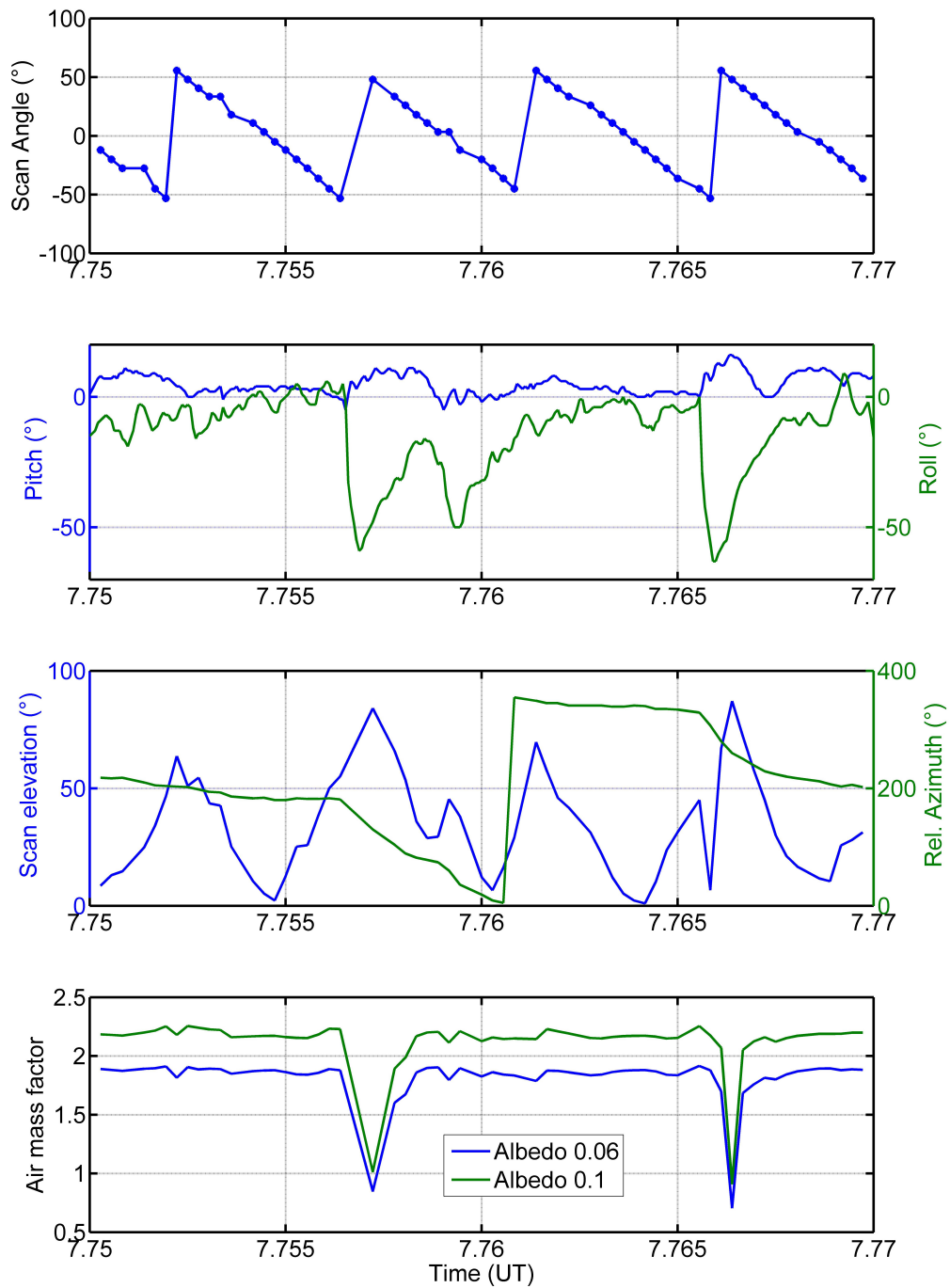


Figure 6. Geometry of the measurements during the test flight (three upper panel) and their simulated effect on the air mass factors for two different ground albedo (lowest panel).

terizations include the optical properties. The polarization response of the spectrometer will be characterized accurately since it is a well-known issues in atmospheric optics based on grating spectrometers. The absolute radiometric calibration of the spectrometer will help us to retrieve the ground albedo from the spectra. A major improvement would consist in using a spectrometer able to measure both NO<sub>2</sub> and SO<sub>2</sub> at the same time. The spectral range of the current SWING system does not permit to study SO<sub>2</sub> absorptions. We are currently looking for an optimal spectrometer, possibly also using a more sensitive detector.

In the near future, the SWING-UAV observation system will perform further test flights above NO<sub>2</sub> sources, such as power plants or chemical factories in Romania. We have also initiated a project to measure NO<sub>2</sub> and SO<sub>2</sub> from ships. Flying above a city to monitor air quality appears a middle-term project due to legislative issues, but it appears technically feasible and it fits the increasing number of civilian UAV applications.

## ACKNOWLEDGMENTS

This project is supported by the Belgian Science Policy (BELSPO). D.E. Constantins work for this study was supported by the Grant SOP HRD/107/1.5/S/76822 TOP ACADEMIC co-financed from ESF of EC, Romanian Government and Dunarea de Jos University of Galati, Romania. We thank Dirk Schuttemeyer for useful discussions.

## REFERENCES

- [1] Berg, N., Mellqvist, J., Jalkanen, J.-P., & Balzani, J. 2012, *Atmos. Meas. Techn.*, 5, 1085
- [2] Constantin, D., Merlaud, A., Van Roozendael, M., et al. 2013, *Sensors*, 13, 3922
- [3] Cosemans, G. & Mensink, C. 2005, in *Proceedings of the 10th Conference on Harmonisation within Atmospheric Dispersion Modelling for Regulatory Purposes*, Heraklion, Crete, Greece, 206–210
- [4] Danckaert, T., Fayt, C., De Smedt, I., et al. 2012, *QDOAS, Software User Manual*, Belgian Institute for Space Aeronomy, Brussels, Belgium
- [5] De Mazière, M., Van Roozendael, M., & Merlaud, A. 2006, in *ISPRS Archives. Vol. XXXVI-1/W44, Second International Workshop: The Future of Remote Sensing*
- [6] Heue, K.-P., Wagner, T., Broccardo, S. P., et al. 2008, *Atmos. Chem. Phys.*, 8, 6707
- [7] Kowalewski, M. G. & Janz, S. J. 2009, in *Proc. SPIE 7452, Earth Observing Systems XIV No. 74520Q*
- [8] Levelt, P., van den Oord, G., Dobber, M., et al. 2006, *IEEE T. Geosci. Remote.*, 44
- [9] Mayer, B. & Kylling, A. 2005, *Atmos. Chem. Phys.*, 5, 1855
- [10] Merlaud, A. 2013, *Development and use of compact instruments for tropospheric investigations based on optical spectroscopy from mobile platforms* (Presses univ. de Louvain)
- [11] Merlaud, A., Van Roozendael, M., Theys, N., et al. 2011, *Atmos. Chem. Phys.*, 11, 9219
- [12] Merlaud, A., Van Roozendael, M., van Gent, J., et al. 2012, *Atmos. Meas. Techn.*, 5
- [13] Platt, U. & Stutz, J. 2008, *Differential Optical Absorption Spectroscopy: Principles and Applications, Physics of Earth and Space Environments* (Berlin: Springer)
- [14] Popp, C., Brunner, D., Damm, A., et al. 2012, *Atmos. Meas. Techn.*, 5
- [15] Roy, D. P., Devereux, B., Grainger, B., & White, S. J. 1997, *International Journal of Remote Sensing*, 18, 1865
- [16] Schönhardt, A., Richter, A., Krautwurst, S., et al. 2011, in *5th International DOAS Workshop*